Available online at www.sciencedirect.com
SCIENCE DIRECT®
Thin Solid Films 476 (2005) 51–58
thin solid films
www.elsevier.com/locate/tsf

Growth mechanism and characterization of chemical oxide films produced in peroxide mixtures on Si(100) surfaces

S. Petitdidier[a], V. Bertagna[b,*], N. Rochat[c], D. Rouchon[c], P. Besson[a], R. Erre[b], M. Chemla[d]

[a]STMicroelectronics, 850 rue Jean Monnet, 38926 Crolles Cedex, France
[b]Department of Materials Chemistry, CRMD, CNRS-Université d'Orléans, Rue de Chartres, BP 6759, 45067 Orléans, France
[c]CEA/LETI, CEA-Grenoble, 17 rue des Martyrs, 38054 Grenoble Cedex 9, France
[d]LI2C, Université P.&M. Curie, 4 place Jussieu, 75005 Paris, France

Received 27 October 2003; received in revised form 23 March 2004; accepted 2 September 2004
Available online 22 October 2004

Abstract

The growth kinetics of silicon chemical oxides in H_2O_2-containing solutions at various pH values and temperatures was studied by electrochemical impedance spectroscopy (EIS), ellipsometry and X-ray photoelectron spectroscopy. Infrared (IR) spectroscopy was also used to investigate the evolution of the surface chemistry from the initial hydrogen coverage as Si–H bonds to the subsequent oxidation states by analysing the Si–O–Si stretching vibration modes. Successive EIS diagrams obtained as a function of time constituted a series of semicircles indicating that the semiconductor/oxide/electrolyte junction can be modelled as a resistance-capacity (RC) circuit. It was then observed that the resistance term increased with time to almost 1 MΩ cm^2 after 3 h in SC1 solution. It is generally known that, in alkaline solutions such as SC1, the oxidation rate reaches rapidly a steady regime controlled by the interfacial charge transfer reaction and the subsequent dissolution of the generated oxide. Accordingly, a mechanism involving a diffusion process of reactants through the oxide barrier followed by a simultaneous dissolution of the layer is proposed. Likewise, in acidic media such as SC2, even though the solubility is extremely low, we have extended our model based on the competition between the oxidation rate at the surface and the dissolution of the built-up oxide, and thus it was possible to evidence oxide solubility at the nanoscopic scale. In addition, thickness measurements by ellipsometry together with the observed gradual change in the IR spectrum of the Si–O–Si vibration mode were interesting parameters revealing that the oxide growth proceeds simultaneously with an evolution of the structure leading to a more compact and insulating dielectric layer. The whole of the results lead to a model for the oxidation process accounting for the observed structure and complex impedance properties under various conditions of chemical treatment.
© 2004 Elsevier B.V. All rights reserved.

PACS: 73.61–r; 73.40.Mr; 77.55+f; 81.65.M; 82.80.F; 84.37
Keywords: Silicon oxide; Growth kinetics; Silicon surface treatment; Electrochemical impedance; SC1; SC2

1. Introduction

The RCA process, developed by Kern and Puotinen [1,2], is still widely used in semiconductor industry for the surface cleaning of silicon wafers. New improvements are continually developed aiming at a better cleaning efficiency, a lower cost, and a strict control of the environmental regulations [3,4]. After removal of the native oxide with a HF treatment, the resulting Si–H_x hydrophobic surface is successively treated in an alkaline ammonia–hydrogen peroxide mixture called SC1, to oxidize the organic contaminants and generate a thin chemical oxide layer which repels all inorganic particles from the surface by setting the zeta potential of both the surface and the particles. In the next step, an acidic HCl–hydrogen peroxide mixture called SC2 allows the metallic contaminants to be dissolved as complex species and excluded from the surface. The pH value of these solutions is the determining

* Corresponding author. Tel.: +33 2 38 49 48 65; fax: +33 2 38 41 70 43.
E-mail address: valerie.bertagna@univ-orleans.fr (V. Bertagna).

0040-6090/$ - see front matter © 2004 Elsevier B.V. All rights reserved.
doi:10.1016/j.tsf.2004.09.008

factor to optimise the elimination of contaminants, particles, organic or metallic species [5]. Most of the optimisations implemented nowadays aim at increasing the cleaning efficiency and decreasing the chemical cost and consumption, the time of process and the size of the wet bench in clean room. For example, we can quote the use of diluted chemistry and megasonics, and furthermore the introduction of chelating reagents [6]. These treatments lead to a thin chemical silicon oxide layer, before thermal silicon oxide build up.

Because of the down-scaling of the elemental Complementary Metal Oxide Semiconductor (CMOS) components, the thickness of the ultra-thin thermal silicon oxide (12 Å), built upon the chemical one, has to be decreased. But, with such a thin insulating layer, the leakage tunneling current becomes a stringent limiting factor [7]. For the next CMOS generation, other dielectric metal oxide materials, called high-k, will supplant the ultra-thin silicon gate oxide. In both cases, the chemical oxide resulting from the surface preparation step, which is needed to ensure a low interface state density, will bring the top surface bonds and make an interface with the dielectric stack. The impact of its thickness, structure and composition will be the key parameter for the final high-k multi layer dielectric oxide.

The growth kinetics of a silicon oxide layer from a hydrophobic surface has been already studied in aqueous media in the presence of strong oxidants such as ozone, hydrogen peroxide or dissolved oxygen. Gould and Irene, in 1989 [8], investigated by in-situ ellipsometry techniques the chemical reactions involved during the aqueous NH_4OH treatment of silicon surfaces. More recently, in alkaline media such as SC1, Adachi and Utani [9] have reported that the thickness was reaching a limited value after a few minutes because of the quasi equilibrium established between the oxidation process and the oxide dissolution by hydroxide ions. On the other hand, measurements by Ohmi et al. [10] lead to the conclusion that, in H_2O_2 30% at 20 °C, the oxide thickness was initially growing fast and reached a plateau after 1000 min, according to a diffusion control of the oxidation process.

The structure of these oxide films has been studied in terms of the remaining Si–H bonds and the position of the Si–O–Si stretching vibration bands by infrared techniques. Ogawa et al. [11] observed that the density of remaining Si–H surface bonds was five times higher in SC2 or HNO_3 than in SC1 or Caro solution. Using Fourier transform infrared (FTIR) spectroscopy with Si substrate surfaces in contact with a 3% H_2O_2 solution at 20 °C, Sugita and Watanabe [12] detected the coexistence of unoxidized Si–H bonds and oxidized Si–O–Si groups for more than 1000 min. They concluded that the oxidation proceeded through islands generation. The use of more than one wet cleaning treatment was also investigated by Ogawa et al. [13] with FTIR attenuated total reflection spectroscopy (ATR) and FTIR reflection absorption spectroscopy. They concluded that SC2 treatment was very different from the other ones (Caro solution, SC1, HNO_3) and gave no change in the properties of the chemical oxide layers formed with other chemicals.

The Si–O–Si absorption band is composed of two vibrational modes: a longitudinal optical (LO) and a transverse optical (TO) [14]. The position of the LO mode has been extensively discussed in the literature as it is sensitive to the structure of the oxide film. Sugita et al. [15] have found that the position of the LO mode is dependent on the density of the film measured by X-ray reflection. Moreover, Sugita et al. [11] have observed that the position of the LO mode shifted towards higher wave numbers during the oxidation in ozone and H_2O_2 aqueous solutions while the Si–H bonds disappeared.

Electrochemical techniques, and more specifically, electrochemical impedance spectroscopy (EIS) were used to study in situ the kinetics and interfacial reactivity of the silicon oxide growth in SC1 solutions [16,17]. In these papers, we evidenced a more pronounced permeability of the oxide barrier to ions and oxidizing agents in alkaline media, whereas this phenomenon vanished in acidic solutions. This behaviour was assigned to the acido–basic properties of the surface oxide layer, showing the existence of Si–OH bonds which can be ionized as $Si–O^-$ groups in alkaline media, or alternatively be transformed into Si–O–Si bonds by bridging in acidic solutions.

Here, we report the oxidation process of hydrophobic silicon surfaces in peroxide mixtures, SC1 and SC2, as a function of time, pH and temperature. This study was focused on the reactivity, homogeneity and chemical composition of the growing thin oxide layer.

2. Experimental

All samples were p-type silicon (100) wafers from the production line of STMicroelectronics. They were initially treated with a Caro solution followed by a HF/HCl treatment to obtain an hydrophobic hydrogen-terminated surface, following the protocol summarized in Table 1.

Then, the oxidation was comparatively studied in H_2O_2-containing solutions at different pH values and temperatures. The experimental details are listed in Table 2.

Table 1
Summary of the successive steps for samples preparation

Step	Solution	Conditions
Organic removal	Caro	100 cm^3 H_2O_2 in 40 l H_2SO_4 for 5 min
Rinse	DIW (deionized water)	Overflow during 5 min at 50 °C
Native oxide removal and hydrogen passivation	HF/HCl	(1:1:100) during 3 min
Rinse	DIW	Overflow during 5 min at 20 °C

Table 2
List of processes used for surface oxidation

Step	Solution	Conditions	Duration
Oxidation	SC1 ($NH_3/H_2O_2/H_2O$)	(1:1:50) at 20 °C	0.4–210 min
	SC2 ($HCl/H_2O_2/H_2O$)	(1:1:50) at 20 °C and 50 °C	10–290 min
	H_2O_2 (H_2O_2/H_2O)	(1:50) at 20 °C and 50 °C	10–290 min
Final rinse	DIW	Overflow at 20 °C	10 min
Dry		Spinning	

Electrochemical experiments were conducted in an electrochemical cell, specially designed to control several parameters, such as the influence of external light and the effect of solution confinement at the seal junction of the sample with the cell [18], so as to optimise the reliability of the results. The back side of the Si sample, covered with a Ga–In alloy, was connected to an EG and G PAR model 273A potentiostat, and an impedance analyser Solartron 1260. The frequency range was selected from 10 kHz to 0.05 Hz in such a way that a complete impedance diagram was obtained within 2–3 min. This configuration allows the diagrams to be scanned in a short time without change of the oxide dielectric properties during the data recording. Then, the Nyquist plots were modelled in terms of parallel resistance-capacity (RC) loops, which values were determined using the software Zplot that is the internal data processor included in the Solartron device.

The oxide growth kinetics was followed with a Rudolph Fe III ellipsometer with a single wavelength, 632.8 nm, and the thickness was extracted using a refractive index value equal to that of the thermal silicon oxide (n=1.462). We are aware that this value is not very well appropriate in the case of very thin chemical oxide layers [19]. But the choice of this single index was useful to obtain the relative thickness values of the layer as a function of time. A hydrophobic surface resulting from the HF treatment was the zero reference for the ellipsometric measurements, assuming that the contribution of the Si–H bonds to the optical constant was negligible. To check these values, X-ray photoelectron spectroscopy (XPS) measurements using a spectrometer with an AlKα X-ray source were performed. The thickness was determined with the intensity ratio of all the oxidized silicon species detected using the formalism of Yano [20].

An interesting feature of our work is the determination of the silicon consumption during the alkaline and acidic chemical treatments. The technique used in this purpose was thickness measurements by ellipsometry, using silicon-on-insulator (SOI) substrates following the procedure described by Celler et al. [21]. The starting wafer consisted of a 2000 Å monocrystalline Si film that was separated by 4000 Å of thermal SiO_2 from the bulk Si substrate. This thermal silicon oxide layer was acting as a buried layer for the ellipsometric measurements using various wavelengths. The etching rate was derived by measurement of the remaining thickness of the silicon layer after the oxidizing chemical treatment.

The chemistry of the silicon surface and the surface bond vibrations were evidenced by FTIR spectroscopy using specific modes depending on the kind of bonds to be detected. The multiple internal reflection mode was performed to study the evolution of Si–H_x hydrogen coverage during the oxidation process, because this technique is very sensitive to a few surface sites. The vibration modes corresponding to the Si–H_x surface groups were obtained by scanning the IR spectrum ranging between 2000 and 2200 cm^{-1}. ATR was chosen to detect the evolution of the Si–O–Si and Si–OH vibration spectra, ranging in the region near 1200 cm^{-1}. Moreover, the vibration of the SiO–H bond was observed as a broad band in the interval 3200–3500 cm^{-1}.

3. Results

The starting point of this experimental investigation was the result obtained in the following experiment: Successive electrochemical impedance spectroscopy measurements gave clear indications related to the growth of a silicon oxide insulating layer as a function of time by reaction of the naked surface of a silicon substrate with oxidizing reactants such as SC1 or SC2 solutions. For example, the in-situ growth kinetics was followed by electrochemical impedance spectroscopy during 3 h at open circuit potential in the dark in SC1 solution. The results are plotted in Fig. 1. The Nyquist plots are semi-circle shaped and the interface can be modelled as a parallel RC circuit. The capacitance values were found equal to a few $\mu F/cm^2$, typical for a silicon/oxide/electrolyte junction including the capacitance of an oxide dielectric layer a few Å thick. After 3-h duration time, while a surface silicon oxide was formed, the Nyquist plots diameter reached a steady state (Fig. 1a), indicating a resistance term equal to $\approx 4.5 \cdot 10^5\ \Omega$, the surface of the sample being equal to 3 cm^2. Then, keeping the sample inside the electrochemical cell, the surface was thoroughly rinsed with pure deionized water and a new SC1 electrolyte was introduced inside the cell, to examine the influence of a possible aging of the SC1 solution. The shape of the obtained Nyquist plots was almost superimposed to the preceding ones, indicating that the steady state was not related to a possible change of the composition of the solution close to the interface, but really to a surface phenomenon. This feature could be, in a first approximation, related to a mechanism controlled by the diffusion of the oxidizing species through the oxide layer [17].

Moreover, the influence of the solution pH on the same oxide was checked by replacing the SC1 by an SC2 solution. Fig. 1b depicts this experiment exhibiting a dramatic increase of the polarisation resistance of the interface reaching values as high as several $10^7\ \Omega$. Finally, after a few minutes, the electrochemical cell was rinsed anew and filled again with SC1 to reproduce the primitive experimental conditions. This experiment led to the recovery of the original Nyquist plot obtained in a SC1

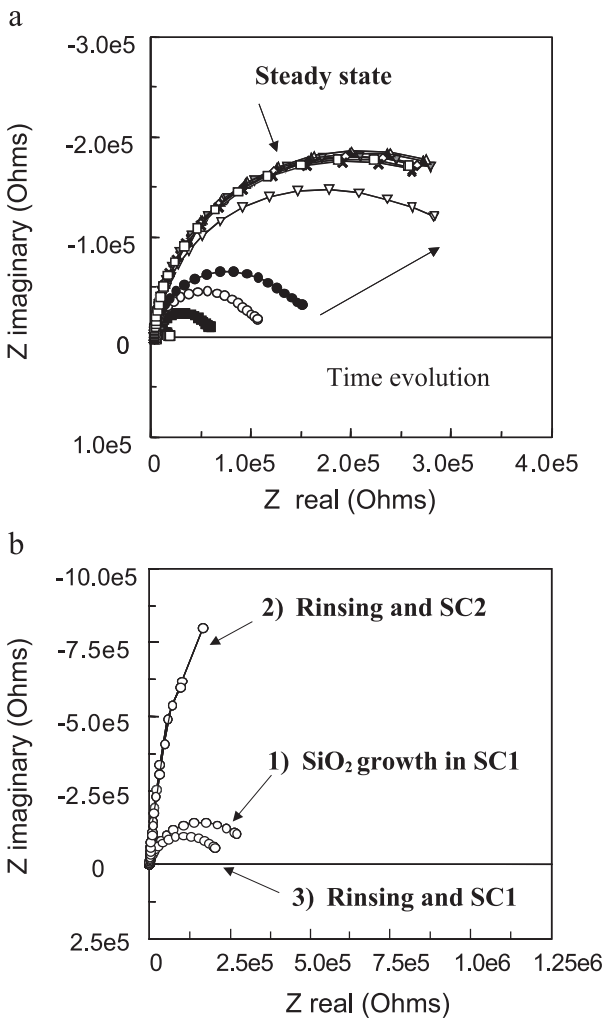

Fig. 1. (a) Successive Nyquist plots recorded on a p-type silicon sample, in a SC1 solution, as a function of time. (b) Nyquist plots recorded on a p-type silicon sample: effect of different treatments on the electrical parameters of the interface. (1) Silicon oxide growth in a SC1 solution, until the steady state is reached, as in (a). (2) Rinsing of the silicon surface in deionised water and addition of a SC2 solution in the cell. (3) Rinsing of the silicon surface in deionised water and addition of a SC1 solution.

solution. We can assume that, during these experiments, the thickness of the chemical silicon oxide did not change significantly. But the polarisation resistance value proved to be extremely sensitive to the pH of the electrolyte solution. In acidic solutions, the oxide layer is transformed into a more compact insulating layer which constitutes a tight barrier against electrical and material transport through it. In fact, experiments of oxide growth in acidic SC2 solutions resulted in a series of semicircles quite similar to those presented in Fig. 1, but the transformation was much slower; the steady state was reached after more than 24 h. We will try to understand these results using other experimental methods.

First, a study of the silicon oxide thickness evolution versus time was carried on both by ellipsometry and XPS. Two distinct behaviours for the chemical oxide growth kinetics were evidenced by ellipsometry as shown in Fig. 2.

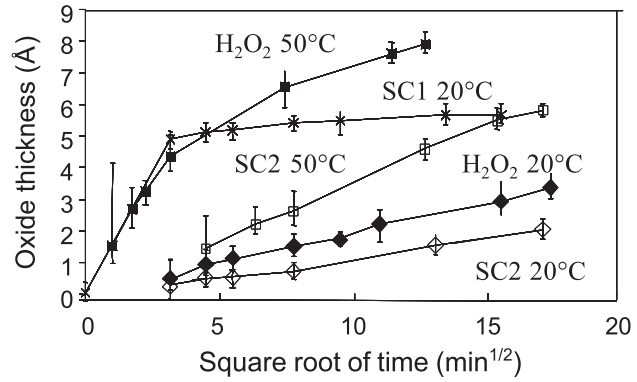

Fig. 2. Optical thickness from ellipsometry vs. time for different process conditions.

As previously mentioned, the growth rate was observed to be much more rapid in SC1 solutions [7,8] than in acidic SC2 or neutral H_2O_2 solutions at the same temperature. However, it is necessary to point out that the quasi equilibrium between the oxidation process and the oxide dissolution in SC1 solutions was reached after only a few minutes and lead to a limiting thickness of the oxide layer in the vicinity of 5–6 Å at 20 °C. So the continual evolution of the polarisation resistance value during 3 h cannot be related to a gradual increase of the oxide thickness.

For this reason, an investigation of the oxide layer structure was undertaken using FTIR spectroscopy. Thus, it was easily recognized that the faster oxide growth recorded in alkaline SC1 solutions was correlated to a fast removal of the hydrogen Si–H_x surface coverage of the primitive hydrophobic samples after treatment by diluted HF. Fig. 3 shows that this first step of the oxidation process was more effective in SC1 at 20 °C than in SC2 or H_2O_2 even at 50 °C.

On the other hand, the structure of the oxide layer can be depicted more precisely by ATR spectroscopy in the region of 1200 cm^{-1} wave number. In the case of a continuous oxide film, the peak corresponding to the Si–O–Si stretching vibration can be split, according to Berreman [22], into two optical modes: LO, in the vicinity of 1200 cm^{-1}, and TO, near 1050 cm^{-1}. We recall that for SC1, the thickness is

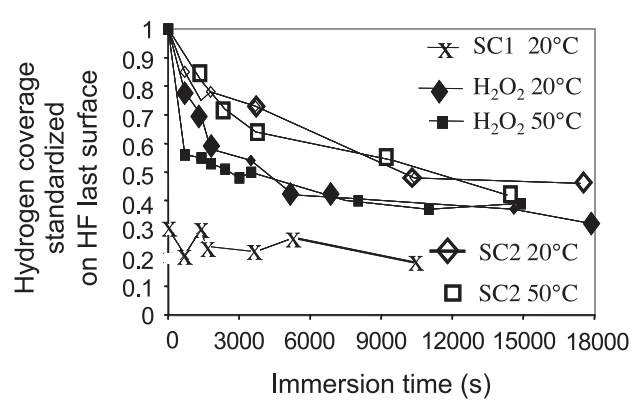

Fig. 3. Time dependence of the Si–H_x hydrogen coverage from MIR spectroscopy vs. different process conditions.

almost immediately higher than one monolayer in correlation with the fast Si–H_x removal rate, and reached a limiting value after a few minutes. Fig. 4 shows that the LO vibration mode appears very early, its intensity increases with time, while the peak shape gets sharper and its position is gradually shifted to a higher energy vibration mode during 3 h. This result indicates that the oxide layer gradually reaches a more compact and well-defined structure, and is consistent with the observed evolution of the polarisation resistance.

An approximately similar behaviour was obtained in acidic SC2 solutions but the evolution rate was extremely slow at room temperature. Then, Fig. 5 shows the successive spectra for the Si–O–Si vibration mode obtained at 50 °C. Compared to the results of Fig. 4, the vibration peaks are broader and coarsely defined, indicating a more complex chemical surface composition. This could be due to the higher heterogeneity of the oxide film composition, with more different surface bonds than in a SC1 oxide. In SC2 at 50 °C, the LO mode appears only after 150 min, when the thickness reaches 3.1 Å, i.e. when the oxide film is thicker than one monolayer determined by both XPS and ellipsometry, indicating that the oxide cannot be considered as a continuous film. These results let us to suggest a non-uniform growth mechanism in SC2, with remaining non-oxidized Si–H_x bonds on the surface. The Si–H_x bonds are extremely stable in acidic media. First, Si–OH groups resulting from the oxidation of Si–H_x bonds appear, yielding to the appearance of the TO mode. Subsequently, the Si–Si back bonds linked to the Si–OH groups are predominantly oxidized because of the polarization of these Si–Si bonds induced by the oxygen atoms. Such results are quite consistent with the conclusion of Sugita and Watanabe [12] indicating that the oxide growth proceeded via the primary generation of surface islands. Only after a long immersion time, it gives rise to a uniform oxide film with limited non oxidized regions and an increase of the oxide thickness.

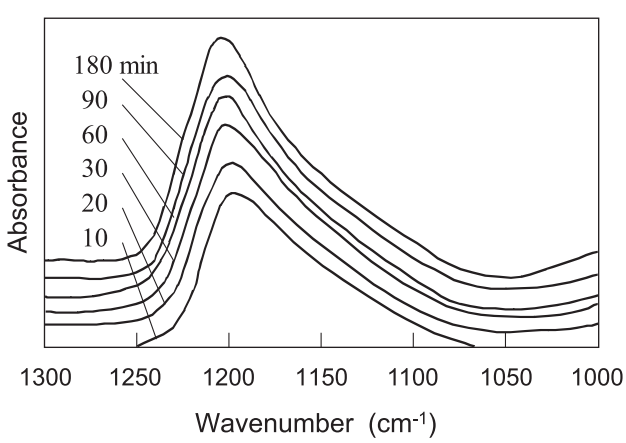

Fig. 4. ATR spectra of the Si–O–Si stretching vibrations in SC1 recorded during 3 h at 20 °C.

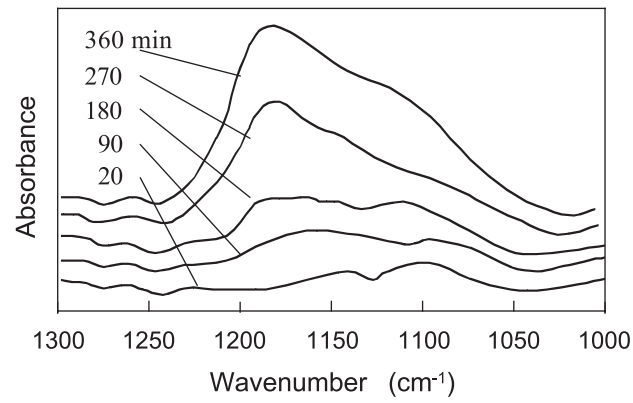

Fig. 5. ATR spectra of the Si–O–Si stretching vibrations in SC2 at 50 °C.

Finally, our experiments based on SOI techniques led us to a sound demonstration of the mechanism oxidation/dissolution controlling the surface Si oxide growth. When a silicon oxide is generated in a peroxide mixture, either acidic or basic, a dissolution process occurs at the same time. This phenomenon was quantified at the angstrom scale using the SOI technique by measurement of the remaining silicon thickness. For example, Fig. 6 depicts the consumed silicon substrate thickness on top of the SOI structure, as a function of various immersion times in a SC1 solution at 20 °C. Although the thickness of the silicon oxide built up on top of the substrate has reached a constant value, the remaining silicon thickness decreased. Considering that the system attained a steady regime of oxidation/dissolution mechanism, this experiment gives access to the chemical silicon oxide etch rate. Such a kind of procedure was also carried on with a thick thermal silicon oxide and led to the results depicted on Fig. 6, which show that the etch rate of the thermal oxide is below that of the chemically grown oxide. At this stage, we recall that the silicon layer constituting the SOI chip was deposited by chemical vapor deposition and has probably not the same structure as the monocrystalline silicon substrate. Then, the etch rates could be not identical for these two kinds of materials. Table 3 shows quantitative results, related to the silicon etch rate in SC1, SC2 and H_2O_2,

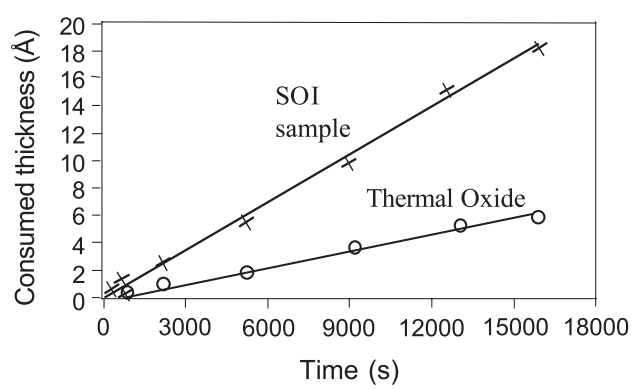

Fig. 6. Consumed silicon oxide thickness versus time reached with the SOI technique.

Table 3
Calculated parameters for the diffusion/reaction model from SOI technique experimental data processing

Solution	Temperature (°C)	Silicon etch rate (Å/min)	d_∞ (Å)	D (cm^2/s)
SC1	20	0.09±0.005	5.8	5.9×10^{-12}
SC2	20	0.008±0.002	2.5	1.2×10^{-12}
	50	0.034±0.004	6.8	3.5×10^{-12}
H_2O_2	20	0.005±0.001	7	6.0×10^{-13}
	50	0.016±0.003	7.5	7.0×10^{-12}

obtained using the SOI technique. These experiments demonstrated that an oxide solubility (in Å/min) was detectable even in acidic media. It is extremely low, 10 times less, as compared to alkaline solutions such as SC1.

4. Discussion

From our experimental results, the oxide growth apparently followed a parabolic law in the case of peroxide mixtures with acidic species (SC2) or neutral pH (H_2O_2), since the thickness was approximately linear versus the square root of time (Fig. 2). The same conclusion holds in the case of SC1 during the initial period preceding the steady regime leading to a plateau. We note that a thickness less than one monolayer, around 3 Å, is recorded even after 5 h in SC2 at 20 °C, 4 h in H_2O_2 at 20 °C and 1 h in SC2 at 50 °C. The XPS measurements were in a good agreement with these results, indicating a thickness less than one monolayer. In such acidic solutions and at this scale of time, the oxide growth is extremely slow and the thickness does not reach a plateau in agreement with the results obtained by Ohmi et al. [10]. We recall that, according to the basic model of oxide growth originally established by Wagner and Grunewald [23], the parabolic law is a result of rate control by diffusion of the reactants through the pre-existing layer as well as by field assisted transport of ionic species. This model was later improved by Deal and Grove [24] who introduced additional terms accounting for the presence of an initial oxide layer, which leads to the linear-parabolic growth process.

De Smedt et al. [25] have extensively described the field assisted growth of the chemical oxide generated in ozonized water and concluded that the mechanism could be fitted more closely using the Fehlner formalism [26] than with the Deal and Grove model [24] based on a pure diffusion phenomenon. They indicate that the diffusion of the reacting species is not the main transport mechanism; a field-assisted drift, where anions can migrate through the oxide film under the influence of an electrical field, should come into play. Due to the oxygen species adsorbed on the silicon surface, a potential drop appears, between the oxidized species and the bulk of the substrate. This potential is constant through the oxide but the electrical field over the oxide layer, calculated as the potential to thickness ratio, can reach extremely high values in the case of ultra-thin insulating layers, which leads to a logarithmic dependence of the thickness versus time. Then, the growth kinetic could be modelled could be well represented with the expression (1):

$$d = E\ln(1 + Ft) \quad (1)$$

where E and F are adjusted parameters proportional to the penetration depth of the species and to the concentration of the precursors, respectively. In Fig. 7, the experimental thickness of the oxide layers, obtained after SC2 or H_2O_2 treatments, were plotted versus immersion time. Both models, Deal and Grove and Fehlner–Mott were superimposed to the experimental curves. Even though Eq. (1) seems to match the oxide growth kinetics in SC2 and H_2O_2, it was difficult to assign a physical meaning of the adjusted parameters E and F derived from the experimental values. The E and F values were calculated for each solution and listed in Table 4.

In fact, although the experimental results indicate that an increase of the temperature leads to a larger oxide thickness, we observed that the term E, related to the penetration depth of the species, did not vary accordingly. As an example, E parameters calculated with H_2O_2 are almost identical at 20 or 50 °C, although the experimental oxide thickness values differ each other by a factor of two.

We now point out that generally these models are appropriate to the oxidation mechanism in a dry atmosphere and none of them accounts for a dissolution process in a liquid phase. For SC1 solution, we already assumed that the growth kinetic was controlled by the diffusion of the species, alternatively by field assisted transport, through the oxide layer, but with an additional term K related to the dissolution rate of the oxide [17,18]. This mechanism leads to a parabolic law during the first stages of the growth and tend to a plateau corresponding to the steady regime oxidation/dissolution. This can be extended to other peroxide mixtures; the differential equation describing this phenomenon is:

$$\partial d/\partial t = D_1 C^0/d - K \quad (2)$$

where d is the thickness, D_1 is a constant proportional to the diffusion coefficient of the species, C^0 is the concentration

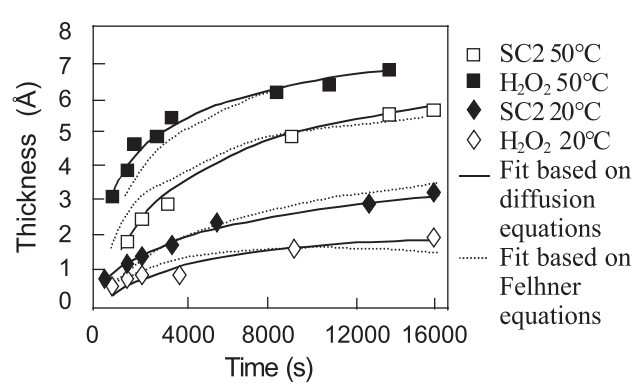

Fig. 7. Comparison of the time dependence between the optical thickness and the fits with the Fehlner or diffusion formalisms.

Table 4
Relevant parameters of Fehlner equation related to the silicon oxide growth in SC2 and H_2O_2 solution

Solution	Temperature (°C)	E (Å)	F (s^{-1})
SC2	20	1.1	2×10^{-4}
	50	2.3	7×10^{-4}
H_2O_2	20	1.5	5×10^{-4}
	50	1.3	1.2×10^{-2}

of H_2O_2 in the bulk of the solution and K is the constant related to the dissolution rate per surface unit. The integration of Eq. (2) leads to:

$$d + \left(D_1C^0/K\right)\ln\left\{1 - \left(K/D_1C^0\right)d\right\} = -Kt \quad (3)$$

It is interesting to check that, at very short time, the development of the logarithmic term to the second order leads to the expected parabolic law:

$$d^2 = 2D_1C^0t \quad (4)$$

Eq. (2) also shows that at infinite time, the thickness will reach a limiting value d_∞ corresponding to the quasi equilibrium state of the oxidation/dissolution process.

$$d_\infty = D_1C^0/K \quad (5)$$

From these equations, the diffusion coefficients D_1 and d_∞ can be obtained as reported in Table 4. We can see that, as expected, D_1 increases with temperature and pH. As shown in Fig. 7, the ellipsometric measurements are in line with this model.

In order to interpret the fast oxide growth recorded in SC1, we proposed in a previous publication [17], a purely electrochemical oxidation mechanism, and suggested the following equations under the zero current conditions for the electron transfer between surface sites and the reactants in solution.

$$Si_{(surface)} + 2OH^- \Rightarrow Si(OH)_{2(surface)} + 2e^- \quad (6)$$

This generation of electrons is compensated by the simultaneous reduction of hydrogen peroxide.

$$H_2O_2 + 2e^- \Rightarrow 2OH^- \quad (7)$$

Alternatively, this reaction could be written:

$$H_2O_2 \Rightarrow 2OH^- + 2h^+. \quad (8)$$

These reactions generate Si–OH surface groups, leading to a passive oxide layer with the condensation of hydroxyl bonds. In the same time, the silicon surface is continually refreshed as a consequence of the quasi equilibrium, between growth and dissolution. Thus the protecting properties of the oxide passive is maintained throughout the whole process.

Nevertheless, it is worth to indicate [17] that, in a pure deaerated ammonia solution under the zero current conditions, the cathodic reaction will only concern the water molecules and result in H_2 evolution or the formation of Si–H bonds.

$$Si_{(surface)} + H_2O + e^- \Rightarrow Si\text{–}H_{(surface)} + OH^- \quad (9)$$

Such a mechanism leads to the formation of hydrophobic Si–H sites at the interface between the Si substrate and the Si oxide passivating layer, and contributes to loosen its protecting properties, thus leading to the appearance of corrosion pits. The remaining quantity of Si–H_x bonds during the oxidation in SC1 solution could result from the local depletion of H_2O_2 molecules due to its high reactivity and decomposition in ammonia solutions.

From our experimental results, an additional surface reaction controlling the oxidation rate is the partial acido–basic dissociation process for the generated silanol groups:

$$\text{–Si(OH)}_2 \Rightarrow \text{–Si}\begin{matrix}\diagup \text{OH} \\ \diagdown \text{O}^-\end{matrix} + H^+ \quad (10)$$

These ionized chains are highly hydrophillic, thus leading to an easy diffusion of the species, H_2O_2 and H_2O, through the oxide thin film and a higher electrical conductance of the layer. This could be the reason why a steady state regime is established within a rather short time during SC1 treatment.

Nevertheless, we can assume that the surface acidity of Si–OH groups is extremely weak, so that the fraction of ionized sites is very small. Indeed, if we recall that the resistance of the layer 5 Å thick is ≈ 1 MΩ cm^2, the order of magnitude of this oxide bulk resistivity is a few 10^{13} Ω cm. Then the remaining Si–OH groups will easily interact together to generate more tightly bound Si–O–Si bridges. This mechanism was clearly supported by the continuous increase of the LO vibration mode of these bonds obtained by ATR spectroscopy. This LO peak is getting sharper with time and is shifted from 1195 to 1205 cm^{-1} as the immersion time increases from 10 to 180 min indicating a better organisation of the oxide film. As a comparison, the frequency of the LO peak for thin thermally oxidized SiO_2 films is in the vicinity of 1250 cm^{-1}. As a conclusion, the continuous evolution during 3 h observed on Nyquist diagrams obtained in alkaline SC1 solutions cannot be related to an increase of the silicon oxide thickness, but to an evolution of the surface chemistry with the condensation of Si–OH species giving rise to a more compact and insulating structure induced by Si–O–Si bridging [27].

The experimental section also showed that the further acidification using SC2 solution lead to a completely passivated surface, because of the neutralization of the negatively charged sites Si–O^- by protons, and followed by the condensation of neutral $Si(OH)_2$ into more tightly bound Si–O–Si bridges. This behaviour is responsible for the sudden increase of the polarization resistance value, which

was observed by electrochemical impedance spectroscopy experiments.

Finally, as shown in Figs. 2 and 3, both the hydrogen surface coverage removal and the oxide growth in acidic SC2 and neutral pure H_2O_2 were extremely slow as compared to the same processes occurring in SC1 solution. Such a behaviour was already pointed out in previous publications [11] and, according to Niwano [28], a residual Si–H_x bonds of 40% was observed even after a few hours, which was interpreted as an enhancement of the Si–H_x stability in acidic media because of the hydrogen exchange with the solution. Moreover, the more compact and insulating structure of the generated oxide acts as a barrier to the transport of both reactants and ions through the layer This situation not only results in an extremely low oxidation rate, but necessarily promotes a lateral growth of the initial nuclei, i.e. a propagation oxide coverage proceeding through islands formation [13].

5. Conclusion

The analysis by electrochemical impedance spectroscopy was very sensitive to reveal the dielectric behaviour of the oxide insulating layer at the surface of a silicon substrate, and more specifically to the chemistry of the surface oxide, depending on its acido–basic properties. All facts were checked by various other complementary techniques such as ellipsometry and IR spectrometry. The growth of chemical oxides in peroxide mixtures was modelled by a mechanism involving the transport of species through the oxide layer corresponding to the conditions of the parabolic law, but complemented by a simultaneous dissolution process leading to a limiting constant thickness due to the appearance of a steady state regime. As a consequence, it was possible to detect the solubility of Si chemical oxide in acidic solutions at the nanoscopic scale always neglected in previous studies. It was thus possible to extract relevant parameters helpful for an optimisation of the processing conditions to obtain a thin and uniform silicon oxide layer. We confirmed that chemical oxides are growing uniformly and more rapidly in alkaline SC1 solutions. On the other hand, during the growth in acidic SC2 solutions, non oxidized regions were clearly detectable at room temperature, thus indicating a mechanism involving the spreading of oxide islands.

We have also pointed out that refining the IR-ATR results in the Si–O–Si stretching vibrations area allows the qualitative control of the uniformity and the structure of the oxide layer. One of the goal of the future cleaning treatments is to improve the atomic structure of the surface, which concerns both the complete Si–H_x removal and, in the same time, the possible control of the silicon oxide thickness at a few angstroms scale. Moreover, the surface structure of this oxide could be an important parameter for the build up of the future multi-component high-k dielectric layers.

Acknowledgements

The authors would like to acknowledge financial support of STMicroelectronics and CEA/LETI for technical assistance.

References

[1] W. Kern, D.A. Puotinen, RCA Rev. 31 (1970) 186.
[2] W. Kern (Ed.), Handbook of Semiconductor Wafer Cleaning Technology, Noyes Publications, New Jersey, 1993.
[3] S. Ojima, K. Kubo, M. Kato, M. Toda, T. Ohmi, J. Electrochem. Soc. 144 (1997) 1482.
[4] R. Sugino, Y. Okui, M. Shigeno, S. Ohkubo, T. Katasaki, T. Ito, J. Electrochem. Soc. 144 (1997) 3984.
[5] L. Sang Woo, Jpn. J. Appl. Phys. 42 (8) (2003) 5002.
[6] F. Tardif, T. Lardin, R. Novak, Solid State Phenom. 65/67 (1999) 19.
[7] B. Brar, G.D. Wilk, A.C. Seabaugh, Appl. Phys. Lett. 69 (18) (1996) 2728.
[8] G. Gould, E.A. Irene, J. Electrochem. Soc. 136 (4) (1989) 1108.
[9] S. Adachi, K. Utani, Jpn. J. Appl. Phys. 32 (9A) (1993) L1189, (part 2).
[10] T. Ohmi, T. Isagawa, M. Kogure, T. Imaoka, J. Electrochem. Soc. 140 (3) (1993) 804.
[11] H. Ogawa, N. Terada, K. Sugiyama, K. Moriki, N. Miyata, T. Aoyoma, R. Sugino, T. Ito, T. Hattori, Appl. Surf. Sci. 56–58 (1992) 836.
[12] Y. Sugita, S. Watanabe, Jpn. J. Appl. Phys. 37 (1998) 3272.
[13] H. Ogawa, K. Ishikawa, S. Fujimura, J. Electrochem. Soc. 143 (1996) 2995.
[14] N. Rochat, A. Chabli, F. Bertin, M. Olivier, C. Vergnaud, P. Mur, J. Appl. Phys. 91 (8) (2002) 5029.
[15] Y. Sugita, S. Watanabe, N. Awaji, Jpn. J. Appl. Phys. Part 1 35 (10) (1996) 5437.
[16] V. Bertagna, R. Erre, F. Rouelle, M. Chemla, S. Petitdidier, D. Lévy, Electrochim. Acta 47 (2001) 129.
[17] V. Bertagna, R. Erre, F. Rouelle, D. Lévy, S. Petitdidier, M. Chemla, J. Solid State Electrochem. 5 (2001) 306.
[18] V. Bertagna, F. Rouelle, M. Chemla, J. Appl. Electrochem. 27 (1997) 1179.
[19] Y.B. Wang, P. Han, Q. Chen, M. Willander, J. Appl. Phys. 82 (1997) 5868.
[20] F. Yano, A. Hiraoka, T. Itoga, K. Kanehori, Y. Mitsui, J. Vac. Sci. Technol., A, Vac. Surf. Films 13 (6) (1995) 2671.
[21] G.K. Celler, D.L. Barr, J.M. Rosamilla, Electrochem. Solid-State Lett. 3 (1) (2000) 47.
[22] D.W. Berreman, Phys. Rev. 130 (6) (1963) 2193.
[23] C. Wagner, K. Grunewald, Z. Phys. Chem., B Chem. Elem. Proz. Aufbau Mater. 40 (1938) 455.
[24] B.E. Deal, A.S. Grove, J. Appl. Phys. 36 (1965) 3770.
[25] F. De Smedt, C. Vinkier, I. Cornelissen, S. De Gendt, M. Heyns, J. Electrochem. Soc. 147 (3) (2000) 1124.
[26] F.P. Fehlner, N.F. Mott, Oxid. Met. 2 (1) (1970) 59.
[27] S. Petitdidier, F. Guyader, K. Barla, D. Rouchon, N. Rochat, R. Erre, V. Bertagna, Cleaning Technology in Semiconductor Device Manufacturing VII, San Francisco, USA September 1–8, 2001, Proc., Electrochem. Soc., 26, 2001, p. 205.
[28] M. Niwano, Surf. Sci. 427–428 (1999) 199.